REDD PILOT PROJECT IN CAMEROON MONITORING FOREST COVER CHANGE WITH EO DATA

Article

6 authors, including:

Manuela Hirschmugl
Joanneum Research Forschungsgesellschaft mbH
34 PUBLICATIONS **488** CITATIONS

SEE PROFILE

REDD PILOT PROJECT IN CAMEROON
MONITORING FOREST COVER CHANGE WITH EO DATA

M. Hirschmugl [a], A. Maier [a], S. Haas [a], R. Siwe [b], M. Schardt [a], J. A. Amougou [c]

[a] JOANNEUM RESEARCH, Wastiangasse 6, A-8010 Graz, email: manuela.hirschmugl@joanneum.at
[b] GAF AG, Arnulfstrasse 197, Munich, Germany
[c] Ministry of Environment and Nature Protection, Yaounde, Cameroon

KEY WORDS: forest monitoring, REDD, deforestation, forest degradation, satellite imagery, classification

ABSTRACT: (50-100 WORDS)

Reducing Emissions from Deforestation and Degradation in developing countries (REDD) is a mechanism for the post-Kyoto reporting as avoiding deforestation is considered to be a contribution to the reduction of green house gas (GHG) emissions. The overall aim of this REDD pilot project in Cameroon is to establish baseline projections of emissions caused by deforestation using Earth Observation combined with regional projections of degradation nested in a wall-to-wall approach. Multi-temporal satellite data and in-situ information is used for the deforestation mapping, which involves a series of pre-processing and processing steps. State-of-the-art methods for mapping forest degradation are tested.

1. INTRODUCTION

At the UNFCCC and Kyoto Protocol Conference of Parties (COP) meeting in Montreal, 2005, the governments of Papua New Guinea and Costa Rica, supported by Latin American and African countries, submitted a proposal for the consideration of reducing emissions from deforestation and degradation in developing countries (REDD) as a mechanism for the post-Kyoto reporting. Avoiding deforestation is considered to be a contribution to the reduction of green house gas (GHG) emissions. Parties agreed to a two-year process of evaluation of the issue by initiating REDD pilot projects to better understand the REDD process. Under the auspices of the European Space Agency (ESA) GMES Service Element on Forest Monitoring a pilot project was developed for REDD implementation and testing in Cameroon with user consultation and endorsement. The REDD pilot project in Cameroon is composed of five components (Technical Proposal) of which the estimation of deforestation and forest degradation from Earth Observation data is one. In the context of the REDD process, forest degradation is considered a bigger threat than deforestation in the Congo Basin. Central African countries are urging that compensation for avoided forest degradation be on equal footing with avoided deforestation. It is thus important to develop and test methods to detect and map forest degradation.

1.1 Aims

The overall aim of the REDD pilot in Cameroon is to establish baseline projections of emissions caused by deforestation (using Earth Observation) combined with regional projections of degradation nested in a wall-to-wall approach. In order to assess deforestation and degradation at a national level a two tier remote sensing analysis to provide forest area maps and forest cover change maps at specific time periods of 1990-2000-2005 using high resolution data for the whole country was proposed. This paper presents an overview of the methodology developed to monitor deforestation and forest degradation in Cameroon.

1.2 Overview of existing work

The GOFC-GOLD Sourcebook on REDD (GOFC-GOLD, 2008) and IPCC guidelines (IPCC, 1996) have a set of recommendations for monitoring deforestation and forest degradation using EO data. Several methodological studies for the REDD process are currently underway in tropical rainforest countries. Deforestation mapping from coarse to medium resolution data (e. g. Hansen & De Fries, 2004) is useful for mapping large deforestation patterns, but not capable of mapping small forest area changes, common in Central Africa. A wall-to-wall example of a study using high resolution satellite data is the one being undertaken in the pacific island state of Vanuatu (Herold et al. 2007). In this study, the deforestation between 1990 and 2000 was assessed using Landsat, Spot and Aster data. The approach consists of several pre-processing steps such as co-registration, image mosaicking, water and cloud masking and image normalization. The main procedure is a wall-to-wall deforestation approach on a pixel basis with manual interaction.

The second similar work has been done in Bolivia (Steininger et al. 2001; Killeen et al. 2007) also based on Landsat imagery. The time span was from the mid-1980ies until 2005 with a focus on the Santa Cruz department and thus was not a full country wall-to-wall mapping. Also, the mapping is restricted to the forest zone with a precipitation of more than 1000 mm per year. The procedure was a pixel-based mapping with a common pixel size of 60 m. A classification of different forest types and also other land cover classes was performed. Training and evaluation was based on field trips and aerial surveys.

In contrast to wall-to-wall mapping, also sampling-based approaches based on high resolution (Landsat) data have been used, e. g. by Duveiller et al. (2008) for Central Africa.

Aside from projects specifically targeted at REDD, many scientific studies are available for each of the processing steps necessary within one implemented REDD processing chain. Since a full review on all this literature would go far beyond the scope of this paper, only the state of the art on the three selected topics are discussed in more detail here. The first topic is

dealing with cloud and cloud shadow detection. This is a crucial pre-processing step when dealing with optical remote sensing data in tropical regions. It is almost impossible to receive a cloud free full coverage, let alone several coverages over time. Therefore a straightforward processing is needed to mask out the areas affected by clouds. The second topic similarly important for large area wall-to-wall mapping is radiometric adjustment. This is necessary in order to mosaick and thus process more than one image at a time. The third topic focussed on here is forest degradation. As already mentioned in the introduction, forest degradation is equally or even more important than deforestation, both in terms of area affected and in terms of GHG emissions.

(1) According to Ricciardelli et al. (2008), two types of **cloud detection** methods can be distinguished: (a) physical methods consisting of multi-spectral threshold techniques applied to single pixels and (b) statistical methods, such as artificial neural networks and pattern recognition techniques, based on the training of textural and spectral parameters.

One approach belonging to the first group was developed at USGS (Hollingsworth et al., 1996; Irish, 2000) for ETM+ imagery. The so-called 'Automatic Cloud Cover Assessment Algorithm' employs radiance thresholds in several bands to separate cloudy from non-cloudy pixels. Each scene is treated separately to minimize the effects of cloud variability.

Another physical method utilizes thermal bands to extract the cloud pixels from MODIS data (Chang et al., 2001).

Christodoulou et al. (2003) applied a statistical method of cloud classification to METEOSAT7 scenes. They classified different types of clouds by combining a neural network self-organized feature map (SOFM) classifier with a statistical KNN classifier.

Compared to cloud detection, far less work has been done for cloud shadow masking. Varlyguin et al. (2001) applied a principal component analysis to various bands of Landsat-7 ETM+ imagery and extracted cloud and cloud shadow masks by combining the first two components of different bands. Another approach for creating a cloud shadow mask by means of all seven MODIS land spectral bands is described in Luo et al. (2008). The shadow is calculated geometrically by assuming that a cloud pixel has a potential height between 0.5 km and 12 km. As in that case far too many pixels are detected as cloud shadows, the geometric solution is combined with the ratio of B6/B3 or B2/B3, as the cloud shadow reflectance is high for the blue band (B1).

(2) **Radiometric adjustment** is necessary in order to use more than one scene at a time. Different methods of relative normalization have been tested. The most common methods are Histogram Matching (LEICA GEOSYSTEMS, 2005) and Linear Regression. As far as the latter is concerned, it is crucial to exclude the obviously changed pixels, otherwise the transformation parameters would be distorted. There are different methods to detect these changes, such as Multivariate Alteration Detection (MAD), which is based on the established canonical correlations analysis (Nielsen et al., 1998) or an iteratively re-weighted modification of the MAD transformation (Canty & Nielsen, 2008). Other methods are based on a number of target objects in the overlap area, on a kNN-cross-validation procedure (Koukal et al., 2007) or on a principal component analysis (Du et al., 2001).

(3) The need to conduct research on tropical **forest degradation** emerged in the 1990s, as the spatial extent of selective logging and fire damage was found to be not accounted for in deforestation studies (Nepstad et al., 1999). Since then forest degradation studies are carried out predominantly in the Amazon Basin. Early studies investigated the degradation mapping potential of Landsat imagery by applying visual interpretation (Stone and Lefebvre, 1998; Nepstad et al., 1999); other methods comprise band-by-band and textural analysis (Asner et al., 2002). Promising results were achieved by deriving cover-type fraction images using Spectal Mixture Analysis (Souza and Baretto, 2000). In subsequent studies , the SMA fraction images were combined with contextual analysis which take into account that logging is spatially bound to either logging decks (Souza et al. 2005) or skid trails (Asner et al., 2005). Among others, Stone and Lefebvre (1998) reported that regardless of the image processing method used, in the third year after the logging event, degraded forest would no longer be distinguishable from intact forest on optical EO imagery.

2. DATA

For the REDD pilot project in Cameroon a full national data coverage from three time periods was obtained. For 1990 and 2000, Landsat data (Landsat 5 and Landsat ETM+ respectively) was purchased. Due to the SLC (Scan Line Corrector) failure (Markham et al. 2004) of Landsat ETM+ in 2003, for 2005 Landsat data is not available without significant data gaps. Thus, DMC (Disaster Monitoring Constellation, http://www.dmcii.com/) data was used alternatively, since it provides a similar geometric resolution (32 m compared to 28.5 m from Landsat) and also the Near InfraRed (NIR) spectral band. The advantage of DMC data can be seen in its large swath width (600 km) and thus a reduced number of images are needed to cover the whole area.

Method development for deforestation mapping and classification into different land cover categories has been done in a first focus area (A) in the centre-east part of Cameroon (45.000 km²). The focus area B serves two purposes: (1) roll-out testing in the more humid zone for the deforestation mapping and in parallel (2) testing of degradation methods. Both areas are shown superimposed on the DMC data in Figure 1.

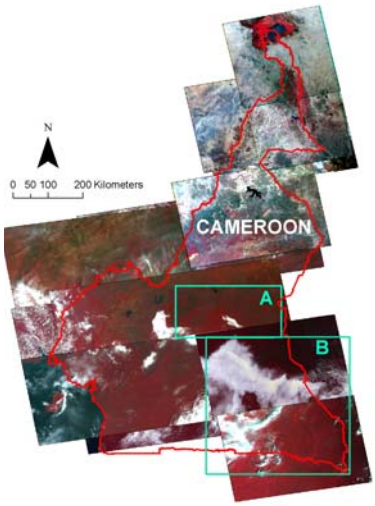

Figure 1: DMC data available for Cameroon superimposed with the two focus areas

3. PREPROCESSING METHODS

The whole pre-processing chain consists of geocoding, cloud- and cloud shadow detection, topographic correction, geometric correction and radiometric adjustment. Geocoding was not necessary, since already geocoded data was acquired. Topographic normalization is necessary for the roll-out on whole Cameroon, since strong topography causes different illumination of the north- and south-facing slopes. This effect

has to be corrected by normalization procedures in all areas with mountainous terrain (Colby, 1991). However, since the focus areas lie in the rather flat to hilly terrain, this pre-processing is not necessary. All remaining pre-processing steps are described in more detail below.

3.1 Cloud and cloud shadow masking

The application of optical remote sensing data in tropical areas often faces the problem of high cloud coverage. Large parts of the data sets used in this study are covered by clouds, haze or cloud shadows: from the 1990 Landsat coverage, about 26%; from the 2000 Landsat imagery approximately 16% and the DMC data had the highest cloud cover with about 28%. In order to deal with the cloud cover a processing was developed to semi-automatically derive cloud and cloud shadow masks. This kind of approach was chosen owing to the patchy appearance of the clouds and the related high cost and time effort of visual delineation. The method consists of 7 steps, they are schematically shown in Figure 2.

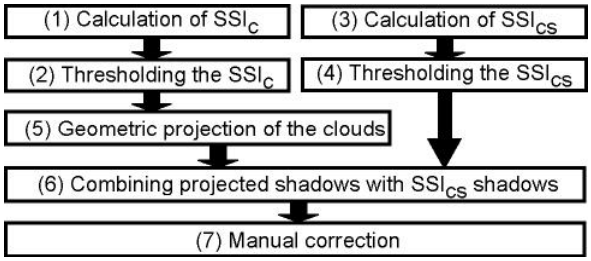

Figure 2: Schematic workflow of cloud and cloud shadow detection

(1) The technique by Wen et al. (2001) was applied using the green and near infrared bands as input for the calculation of a Spectral Separation Index for clouds (SSI_c). The resulting image's histogram shows a bimodal distribution. As the 1st peak indicates cloud pixels and the 2nd cloud-free ones, the next step (2) consists of separating them by simple thresholding. For cloud shadows, no such clear border exists. Therefore another SSI for detecting cloud shadows (SSI_{cs}) is computed which differs from the first SSI only by using a different weighting factor (step 3). The fourth step (4) is again a thresholding procedure, this time based on SSI_{cs}. The result still shows a confusion of cloud shadow areas with spectrally similar areas, such as water bodies or hillsides not facing the sun. This problem is largely solved in steps five and six by computing each cloud's shadow geometrically by means of elevation data, sun position at the time of image acquisition (α and Zd in Figure 3) and measured average cloud height (step 5). In step (6), a region-based analysis determines automatically, whether the spectrally detected shadow fulfils the geometric requirements to be a cloud shadow. If this is not the case, e. g. for lakes, the primarily detected areas are suppressed. In the seventh and final step, the few remaining errors (resulting e. g. from varying cloud heights or from overlapping cloud shadows with water bodies) are removed manually and haze areas are added to the mask (step 7).

The result of these steps is a mask of all areas which cannot be used in the further processing. Other data sources have to be explored to fill these gaps, such as SAR data (Mayaux et al. 2002) or lower resolution optical data like MODIS.

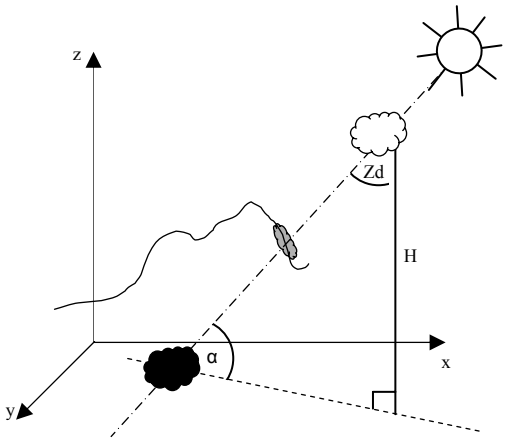

Figure 3: Geometric projection of a cloud onto the terrain

3.2 Geometric adjustment

The original geo-referenced scenes were overlaid to assess their geometrical congruence. Shifts of up to 120 m, especially in W/E direction could be observed in the test area, especially between the Landsat and DMC data. A deforestation mapping based on this data, especially of areas with a lot of small structured (riparian) forest, would result in severe erroneous deforestation on one side and wrongly classified afforestation on the other side. Therefore, the data sets have to be adjusted to ensure congruence and thus correct results. Two different fully-automatic approaches were tested to perform the geometrical adjustment: (1) Coarse registration and (2) Fine registration. The main difference between the two procedures is that fine registration performs local correction, which is important, if the images are internally distorted. In contrast, coarse registration adjusts the whole image with the same polynomial correction. During the first investigation (focus area A), it turned out that with the coarse registration the images could not be fitted into a congruent geometry. Therefore, the fine registration was performed resulting in a stack of three geometrically congruent image data sets.

3.3 Radiometric adjustment

For national coverage of Cameroon, it is not time and cost effective to treat each of the 78 images independently. Therefore, neighbouring images from similar acquisition dates were combined into blocks and made radiometrically comparable. For this radiometric adjustment, the following approaches were tested on the result of the previous steps (excluding clouds and shadows).

(1) Linear regression: Adjustment based on simple linear regression: $x_k^* = a_k x_k + b_k$, where x_k^* is the k^{th} spectral band of the adjusted scene and the coefficients a and b correspond to gain and offset of the best fitting line (LEICA GEOSYSTEMS, 2005).

(2) Histogram Matching uses the histograms of the two overlaps to adjust one image to the properties of the other (LEICA GEOSYSTEMS, 2005)

(3) Regression using Principal Component Analysis (Du et al., 2001). This is the least known method and is therefore discussed in more detail. All pixels, except for clouds and water bodies, are considered initially representative for the linear relationship between all overlap areas of the scenes to be mosaicked. By means of a band-specific PCA only the non-changed pixels of an overlap area are used. The linear relationship is considered to produce a good result, as long as the linear correlation coefficient is greater than 0.9. After this

procedure has been done for all overlap areas, gains and offsets for the whole scenes are calculated, using means and standard deviations of the non-changed overlapping areas, respectively. The last step consists in an overall adjustment, in order to conserve the initial radiometric resolution. If the smallest gain is less than 1, the other gains are divided by it, so that all gains are greater than 1. Offsets are normalized by adding the absolute value of the smallest offset to all others, which is only necessary if the smallest offset is negative. The advantage of this method compared to simple linear regression is that the radiometric resolution is conserved by the overall adjustment. Another positive effect is that this method is independent of the order of compositing. As far as linear regression and histogram matching are concerned, you have to rely on visual inspection to decide which scene you declare as 'good' enough to be the master scene to which all other scenes will be matched.
(4) Linear regression based on non-changed pixels: Here, a PCA was applied to the original overlap areas to find the non-changed pixels (low values in the second PC). Only those were used as input to the computation of the linear regression coefficients.

4. METHOD FOR MAPPING DEFORESTATION

4.1 Image segmentation

Pixel-to-pixel change detection has widely been used in the past. Many different factors influence the final pixel value even if the area is mapped with the same sensor: slightly different viewing angle, geometric shifts, atmospheric effects, phenological effects and sun-position, to name a few of them. In addition, if images (pixels) from different sensors should be compared, there are yet more influencing factors: different geometric resolution (Landsat = 28.5m, DMC = 32m), different spectral resolution (e. g. Landsat ETM+ NIR = 0.775-0.9, DMC NIR = 0.77-0.9), different swath widths with the associated properties (Landsat swath width = 185 km, DMC swath width = 600 km). All those factors, together with still small geometric inaccuracies remaining despite the fine-registration of the images, lead to the fact that most pixel values in question are not directly comparable.
Different illumination, atmospheric effects, phenological properties or spectral resolution of the sensor cannot be changed. However, slight shifts resulting from different viewing angles, different geometric resolution etc. can be taken care of by using a segmentation approach. Existing comparisons between pixel-based and segment-based approaches (Meinel et al., 2001; Whiteside & Ahmad, 2005) also favour segmentation over pixel based analysis. In addition, there are three more advantages of the segment-based approach compared to the pixel-based method: first, the object's information (e. g. area and shape) can be used to suppress objects with a size below the minimum mapping unit or very long and thin segments, which can be attributed to remaining geometric inaccuracies. Second, the scattered appearance of pixels, commonly known as "salt-and-pepper-effect" is avoided. Third, segments can easier be modified than single pixels; this saves considerable time in the control phase applying a manual correction. Segment-based approaches are also used in similar projects (Duveiller et al. 2008). The segmentation procedure used in the current study in Cameroon consists of a series of pre-processing and processing steps, as schematically in Figure 4.

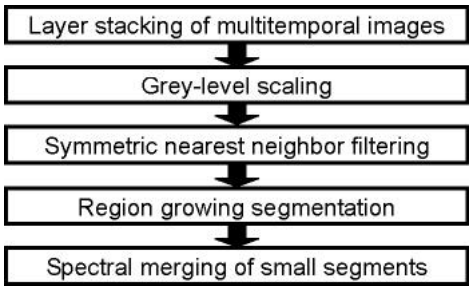

Figure 4: Processing steps for multi-temporal segmentation

First, all three pre-processed images are stacked into one multi-temporal layer stack. In order to balance the weight, from each data set only the bands NIR, red and green are used. Grey-level scaling is necessary to ensure equal conditions for each band and time. Otherwise, one band or one time frame would affect the segmentation more than another. The SNN filtering algorithm maintains the edges, while smoothing the area between edges. Region growing segmentation used here is a standard region growing algorithm with a local and a global threshold to be set by the operator. After segmentation, very small regions are merged with their most similar neighbours. More details on the individual processing steps can be found in Hirschmugl et al. (2008).The result is one single set of segments to be used for the following forest- non-forest differentiation.

4.2 Change detection

Based on the derived segments and the pre-processed data from the individual years, a set of segment attributes is generated including mean NDVI, mean band values and respective standard deviations etc. These attributes are subsequently used to find thresholds to separate forest from non-forest. In a second step, the result is checked visually for errors. Manual correction is comparably easy, since only the segment's attribute has to be changed. Only thereafter, post classification comparison is used to quantify deforestation.

5. MAPPING FOREST DEGRADATION

This study examines the potential of spectral mixture analysis (SMA) based features for mapping forest degradation and regeneration caused by selective logging. Forest ecosystems show a spatially heterogeneous composition of cover types like vegetation and soil. Each pixel of satellite imagery comprises a mixture of these cover types, referred to as endmembers. The premise of SMA is that pixel reflectance is the sum of reflectance for each endmember, weighted by their fractional abundance within each pixel (Asner et al., 2003).
The application of SMA to Landsat data as applied in the current study consists of the following processing steps:
(1) Minimum Noise Fraction (MNF) Transformation (Kruse, 2000) is applied in order to reduce noise and data dimensionality.
(2) Endmember selection: Endmember spectra are derived by using the image feature space. The point cloud in the feature space (scatterplot) of the first and second MNF-band shows a triangular shape. The three vertices of the point cloud represent the endmember positions with maximal abundance of a cover type. Pixels in endmember position are cross-checked in the original image in order to link each endmember to the respective land-cover type. Due to the triangular shape, three endmembers could be identified: Soil, appearing most pure on unpaved logging roads, Green Vegetation (GV) in regrowth

areas or on abandoned logging roads, and Shade in shaded relief positions.

(3) Calculation of endmember fractions C for each pixel using:

$$\vec{a}_{GV}C_{GV} + \vec{a}_{Soil}C_{Soil} + \vec{a}_{Shade}C_{Shade} = \vec{b}$$
$$C_{GV} + C_{Soil} + C_{Shade} = 1$$

where $\vec{a}$ is the endmember vector and $\vec{b}$ is the pixel vector of the first and second MNF-band. For each pixel the sum of the fractions is constrained to one.

(4) The Normalized Difference Fraction Index (Souza et al., 2005) is modified due to the absence of a Non-Photosynthetic Vegetation (NPV) endmember by replacing the term *(Soil + NPV)* with *Soil* only.

$$\text{mNDFI} = \frac{\frac{GV}{1-Shade} - Soil}{\frac{GV}{1-Shade} + Soil}$$

6. FIRST RESULTS AND DISCUSSION

6.1 Cloud and cloud shadow masking

Figure 5 shows the different steps to derive cloud and cloud shadow masks from the scenes. The original (a) shows a water body in the centre of the image, which is spectrally similar to a cloud shadow and therefore detected as one after applying the SSI_{cs} (b). By combining the SSI_{cs} shadow mask with the geometrically computed shadows (c), the dark pattern is detected as a non-cloud shadow and deleted from the final cloud shadow mask. The final cloud and cloud shadow mask is shown in d).

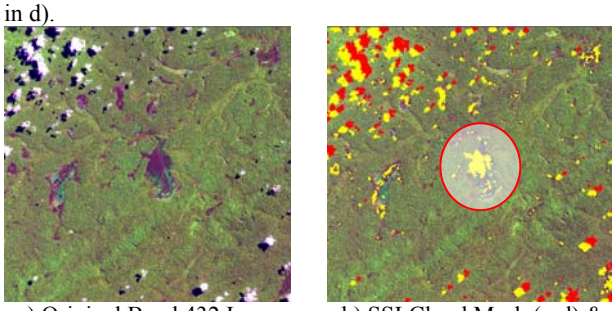

a) Original Band 432 Image

b) SSI Cloud Mask (red) & SSI Cloud Shadow Mask (yellow)

c) Geometrically computed Shadow Mask (orange)

d) Final combined Mask: clouds (red) and cloud shadows (blue)

Figure 5: Cloud and Shadow Masks for a Landsat 5 image

The proposed method is an efficient combination of different approaches to detect and separate cloud and cloud shadow areas from useful image content. However, a final visual check is still needed to remove remaining errors. Yet, the effort compared to a full visual delineation of all this small and scattered clouds and cloud shadows is minimal.

6.2 Radiometric adjustment

The results of the four approaches described in section 3.4 were statistically evaluated based on the comparison of different land cover classes in the overlap area of the two neighbouring images, called image A_{orig} and B_{orig}. The mean was computed separately for each test area of the adjusted image and then compared to the mean of the original master image (A_{orig}). Only in case of method 3, where no master file is used, the difference between both changed image means is used. Figure 6 shows the average difference for bands 3, 4 and 5 calculated based on the forest reference areas. The difference between the original images (red line) is quite large, up to 10 grey values in case of band 3. Such a big difference would certainly lead to problems in a joint classification. The assumption therefore is: the smaller the difference, the better the method works for that specific test area. In the current case, all methods reduce the difference for forest areas to less than two digital numbers. Methods 2, 3 and 4 show quite similar results and from this analysis, no clear preference can be given to any of these methods. In a second step, the same comparison is made for non-forest areas (Figure 7). Here, the results are more diverted with method 3 actually worsening the result compared to the original images. Histogram-matching performs clearly best for non-forest areas in this particular case. However, more different overlaps have to be included in the analysis to confirm this finding.

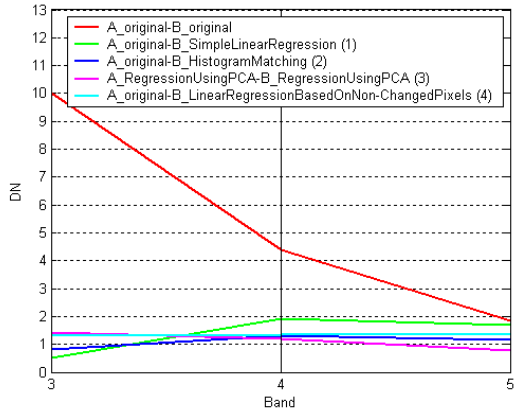

Figure 6: Mean Differences for forest reference areas

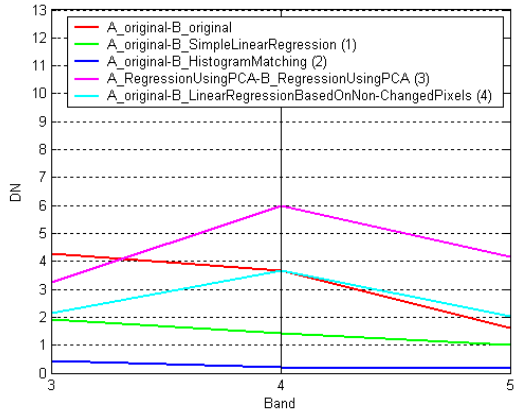

Figure 7: Mean Differences for non-forest reference areas

6.3 Mapping Deforestation

Based on the corrected forest masks for focus area A, two change masks considering both de- and reforestation were derived. The change masks showed a deforested area between

1990 and 2000 of 529.786 km² and a reforested area for the same time span of 441.239 km². From 2000 to 2005, the deforested area is 524.925 km² (see an example area in Figure 8) and the reforested area amounts up to 583.111 km². Between 1990 and 2000, these figures lead to a net loss of 88.547 km² and between 2000 and 2005 to a net gain of 58.186 km². These net change values have to be interpreted with care, as already mentioned by Grainger (2008). Trends can be misinterpreted and a prognosis for the future is very unstable based on such data. A further critical point in GHG budgeting based on net changes only is, that secondary forest might not be binding as much green house gases as the original forest. This can be caused be lower biodiversity, lower plant density or simply a lower average tree size. Therefore, reforestation areas are mapped individually and have to be further analyzed for its contribution to REDD.

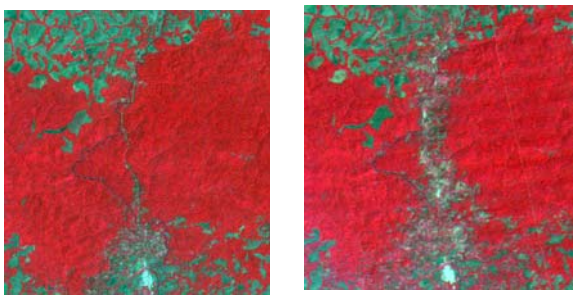

(a) (b)

Figure 8: Comparison of forest appearing red in (a) 2000 (Landsat bands 432) and (b) 2005 (DMC bands 123)

6.4 Mapping Forest Degradation

Interim results show that the mNDFI (Figure 9, top) is sensible to forest degradation (area A). Dark pixels are associated to logging trails and forest areas affected by selective logging activities. The spatial pattern caused by selective logging is also found in the soil fraction image (blue pixels in Figure 9, area A). A similar pattern in neighbouring parts of the image (area B) could be observed in the GV fraction image (red pixels in Figure 9). That leads to the assumption that a regeneration process replaces degradation signals over time.

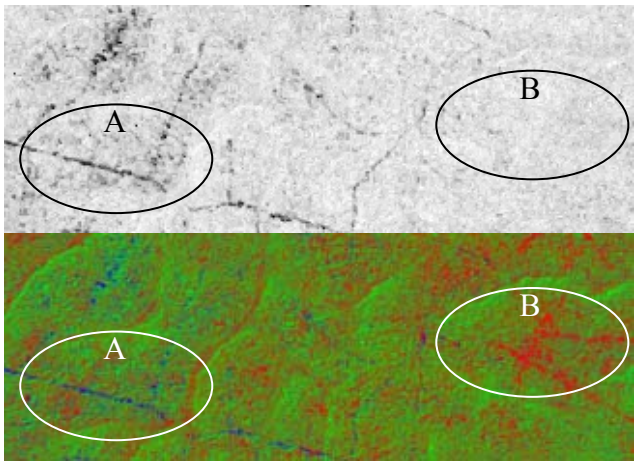

Figure 9: top: mNDFI grayscale image, bottom: Fraction image composite RGB (GV, Shade, Soil)

The SMA-based fraction and mNDFI images are evaluated by comparing the separability of test areas for intact forest, regeneration and forest degradation (including logging trails, logging decks, forest gaps and intact trees in between). The Jeffries-Matusita distance (JM; as given in LEICA GEOSYSTEMS, 2005) serves as a range-independent measurement for relative separability.

Figure 10 involves two topics: (1) the separability of intact, degraded and regenerated forest in the different features (mNDFI, GV, Soil and Shade) and (2) the influence of the spectral band selection. Regarding topic (1), it can be seen that degradation can be best separated in the mNDFI and in the Soil fraction image, while regeneration is best separable in the GV fraction. Regeneration is associated to high NIR reflectance and shows higher separability values than degradation. Regarding topic (2), GV and Shade fractions show similar separability for both spectral subsets a (band 3, 4, 5, 7) and b (band 3, 4), whereas the Soil fraction and the mNDFI show a higher separability for spectral subset a. Hence the degradation mapping potential of sensors with minor spectral resolution like DMC is limited.

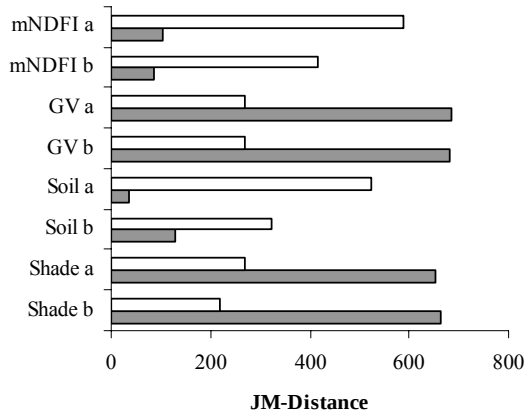

Figure 10: Separability values (JM): white bars for intact forest and degradation; gray bars for intact forest and regeneration, both calculated with two different sets of bands. (a) Landsat bands 3, 4, 5, 7; (b) bands 3 and 4 only.

The intermediate results confirm the previous findings that features indicating forest degradation persist only for up to 2 years. A baseline calculation in a REDD context would require dense time-series of satellite imagery. To overcome this problem regeneration mapping could be taken into account, as it is found subsequent to degradation and more persistent over time. First results of this study indicate that reducing data dimensionality and selecting endmembers in a 2D feature space might provide an adequate approach for a simple and robust mapping of forest degradation.

7. CONCLUSIONS

This paper describes the overall methodology and in more detail three selected topics for the REDD pilot case in Cameroon. Two of the topics deal with pre-processing steps important for large area wall-to-wall mapping: cloud and cloud shadow detection and radiometric adjustment. It could be shown, that the proposed method for cloud and cloud shadow detection is useful and reduces the manual interaction to a minimum.

All four tested relative radiometric adjustment procedures significantly reduced the differences between reference areas of adjacent images, as tested in the overlap area. For forest reference areas, all methods performed similarly, while for non-forest areas, histogram-matching gave the best results.

However, other issues such as the problems with decreased radiometry for linear regression, possibility for automation and the advantages and disadvantages of having a master and several slave images, if a larger amount of images should be processed, have to be investigated before a final conclusion can be drawn.
The third topic investigated is the detection of forest degradation. It could be shown, that by using three instead of four endmembers and the calculation of a modified NDFI, current degradation can be detected. Similar patterns in neighbouring areas indicate that regeneration signals replace degradation signals over time. A field study is needed (has been planned) to verify the results.

8. ACKNOWLEDGEMENTS

The authors would like to thank ESA and GTZ-COMIFAC for financial support and Sharon Gomez and Thomas Häusler from GAF-AG for valuable inputs and technical discussions.

9. REFERENCES

ASNER, G.P., HICKE, J.A., LOBELL, D. B. 2003. Per-pixel analysis of forest structure: Vegetation indices, spectral mixture analysis and canopy reflectance modeling. Remote sensing of forest environments: Concepts and case studies. pp. 209–254.

ASNER, G.P., KELLER, M., PEREIRA, R., ZWEEDE, J.C. 2002. Remote sensing of selective logging in Amazonia Assessing limitations based on detailed field observations, Landsat ETM+, and textural analysis. Remote Sensing of Environment, Vol. 80 No. 3, pp. 483-496.

ASNER, G.P., KNAPP, D.E., BROADBENT, E.N., 2005. Selective Logging in the Brazilian Amazon. American Association for the Advancement of Science, Vol. 310 pp. 480-482.

CANTY, M.J. & NIELSEN, A.A., 2008. Automatic radiometric normalization of multitemporal satellite imagery with the iteratively re-weighted MAD transformation. Remote Sensing of Environment, Vol. 112, pp. 1025-1036.

CHANG, C.W., LIM, K.H., LIEW, S.C., 2001. Cloud Mask for MODIS. Paper presented at the 22nd Asian Conference on Remote Sensing, 5-9 November 2001, Singapore.

CHRISTODOULOU, C.I., MICHAELIDES, S.C., CONSTANTINOS, S.P., 2003. Multifeature Texture Analysis for the Classification of Clouds and Satellite Imagery. IEEE Transactions on Geoscience and Remote Sensing, Vol. 41, No. 11, pp. 2662-2668.

COLBY, J.D., 1991. Topographic normalization in rugged terrain. Photogrammetric Engineering and Remote Sensing, Vol. 57, No. 5, pp. 531-537.

DU, Y., CIHLAR, J., BEAUBIEN, J., LATIFOVIC, R., 2001. Radiometric Normalization, Compositing, and Quality Control for Satellite High Resolution Image Mosaics over Large Areas. IEEE Transactions on Geoscience and Remote Sensing, Vol. 39, No. 3, pp. 623-634.

DUVEILLER, G., DEFOURNY, P., DESCLÉE, B., MAYAUX, P., 2008. Deforestation in Central Africa: Estimates at regional, national and landscape levels by advanced processing of systematically-distributed Landsat extracts. Remote Sensing of Environment, Vol. 112, No. 5, pp. 1969-1981.

GOFC-GOLD Sourcebook on REDD, 2008. Available at: http://www.gofc-gold.uni-jena.de/redd. Last accessed: X 2008.

GRAINGER, A., 2008. Difficulties in tracking the long-term global trend in tropical forest areas. Proceedings of National Academy of Sciences of the United States of America (PNAS), Vol. 105, No. 2, pp. 818-823.

HEROLD, M., SAMBALE, J., LINDNER, M., URBAN, M., WEAVER, S., 2007. Satellite based monitor-ing of the national forest resources in the pacific island state of Vanuatu. DGPF Tagungsband 16 / 2007 – Dreiländertagung SGPBF, DGPF und OVG, pp. 391-398.

HIRSCHMUGL, M., SCHARDT, M., HÄUSLER, T., GOMEZ, S., AMOUGOU, J.A., 2008. REDD pilot project in Cameroon - method development and first results. Proceedings of EARSeL Symposium, June, 2 – 6, 2008, Istanbul, Turkey, in print.

HOLLINGSWORTH, B. CHEN, L., REICHENBACH, S.E., 1996. Automated cloud cover assessment for Landsat TM images. SPIE Conference Proceeding, 2819, pp. 170-179.

IPCC, 1996. Revised 1996 IPCC Guidelines. Available at: http://www.ipcc-nggip.iges.or.jp/public/gl/invs1.html. Last accessed: X 2008.

IRISH, R. R., 2000. Landsat 7 automatic cloud cover assessment. SPIE Conference Proceeding, 4049, pp. 348-355.

KILLEEN, T. J., CALDERON, V., SORIA, L., QUEZADA, B., STEININGER, M., HARPER, G., SOLÓR-ZANO, L. A., TUCKER, C. J., 2007. Thirty years of land-cover change in Bolivia. AMBIO: A Jour-nal of the Human Environment, Vol. 36, No. 7, pp. 600-606.

KOUKAL, T., SUPPAN, F., SCHNEIDER, W., 2007. The impact of relative radiometric calibration on the accuracy on kNN-predictions of forest attributes. Remote Sensing of Environment, Vol. 110, pp. 431-437.

KRUSE, F. A., 2000. Extraction of Compositional Information for Trafficability Mapping from Hyperspectral Data. In Proceedings of SPIE International Symposium on AeroSense, 24 – 28 April 2000, Orlando, pp. 262 – 273.

LEICA GEOSYSTEMS, 2005. ERDAS Field Guide™. Available at: http://www.gis.usu.edu/manuals/labbook/erdas/manuals/FieldGuide.pdf.

LUO, Y., TRISHCHENKO, A.P., KHLOPENKOV, K.V., 2008. Developing clear-sky, cloud and cloud shadow mask for producing clear-sky composites at 250-meter spatial resolution for the seven MODIS land bands over Canada and North America. Remote Sensing of Environment, doi: 10.1016/j.rse.2008.06.010.

MARKHAM, B.L., STOREY, J.C., WILLIAMS, D.L., IRONS, J.R., 2004. Landsat sensor performance: history and current status. IEEE Transactions on Geoscience and Remote Sensing, Vol. 42, No. 12, pp. 2691- 2694.

MAYAUX, P., DE GRAND, G. F., RAUSTE, Y., SIMARD, M., SAATCHI, S., 2002. Large-scale vegetation maps derived

from the combined L-band GRFM and C-band CAMP wide area radar mosaics of Central Africa. International Journal of Remote Sensing, Vol. 23, No. 7, pp. 1261-1282.

MEINEL, G., NEUBERT, M., REDER, J., 2001. Pixelorientierte versus segmentorientierte Klassifikation von IKONOS-satellitenbilddaten – ein Methodenvergleich. Zeitschrift für Photogrammetry, Fernerkundung und Geoinformation 3/2001, pp. 157-170

NEPSTAD, D. C., VERISSIMO, A., ALENCAR, A., 1999. Large-scale impoverishment of Amazonian forests by logging and fire. Nature, Vol. 398, pp. 505-508.

NIELSEN, A.A., CONRADSEN, K., SIMPSON, J.J., 1998. Multivariate Alteration Detection (MAD) and MAF Postprocessing in Multispectral, Bitemporal Image Data: New Approaches to Change Detection Studies. Remote Sensing of Environment, Vol. 64, pp. 1-19.

RICCIARDELLI, E., ROMANO, F., CUOMO, V., 2008. Physical and statistical approaches for cloud identification using Meteosat Second Generation-Spinning Enhanced Visible and Infrared Imager Data. Remote Sensing of Environment, Vol. 112, pp. 2741-2760.

SOUZA, JR. C. M., BARRETO, P., 2000. An alternative approach for detecting and monitoring selectively logged forests in the Amazon. International Journal of Remote Sensing, Vol. 21 No. 1, pp. 173-179.

SOUZA, JR. C. M., ROBERTS, D. A., COCHRANE, M. A., 2005. Combining spectral and spatial in-formation to map canopy damage from selective logging and forest fires. Remote Sensing of Environment, Vol. 98, pp. 329 – 343.

STONE, T.A., LEFEBVRE, P., 1998. Using multi-temporal satellite data to evaluate selective logging in Para, Brazil. International Journal of Remote Sensing, Vol. 19, No. 13, pp. 2517-2526.

VARLYGUIN, D., WRIGHT, R.K., GOETZ, S.J., PRINCE, S.D., 2001. Advances in Landcover Classification for Application Research: A case study from the mid-atlantic RESAC. Proceedings of 'The American Society of Photogrammetry and Remote Sensing'. St. Louis, MO, 7 pages. Available at www.geog.umd.edu/resac. Last accessed: X 2008.

WEN, G., CAHALAN, R. F., TSAY, S.-C., OREOPOULOS, L., 2001. Impact of cumulus cloud spacing on Landsat atmospheric correction and aerosol retrieval. Journal of Geophysical Research, Vol. 106, No. D11, pp. 12:129-12:138.

WHITESIDE, T., AHMAD, W., 2005. A comparison of object-based and pixel-based classification methods for mapping land cover in northern Australia. Proceedings of SSC2005 Spatial Intelligence, innovation and praxis: The national biennial conference of the spatial sciences institute.